The 2014 World Congress on
Advances in Civil, Environmental, and Materials Research (ACEM14)
Busan, Korea, August 24-28, 2014

Structural and Magnetic Properties of Co Doped Iron Oxide Nanoparticles

*Saira Riaz[1)] and Shahzad Naseem[2)]

Centre of Excellence in Solid State Physics, University of the Punjab, Lahore 54590, Pakistan
[1)] saira_cssp@yahoo.com

ABSTRACT

We here report the preparation and characterization of cobalt doped iron oxide nanoparticles using sol-gel method. The dopant concentration is varied as 2%, 4%, 6%, 8% and 10%. The position of diffraction peaks shifts to slightly higher angles due to smaller ionic radii of cobalt as compared to that of iron. No peaks corresponding to cobalt or cobalt oxide are observed indicating that dopant has been successfully incorporated in the host lattice. Cobalt with electronic configuration of $[Ar]3d^7 4s^2$ has one more electron than iron. Cobalt atom donates one d and two s electrons to oxygen that results in remaining six electrons on cobalt. When Co is substituted for Fe with spin down electron the spin down d band gets completely filled with remaining one d-electron residing in spin up band. This results in increase in net magnetization in cobalt doped iron oxide nanoparticles as compared to undoped iron oxide nanoparticles as compared to undoped iron oxide nanoparticles.

1. INTRODUCTION

Due to remarkable potential of iron oxide for various applications, the research on different phases of iron oxide is increasing widely. The precise control of shape and size of iron oxide nanoparticles is gaining attention in order to enhance their applications in data storage devices, as a catalyst, in biomedical applications, in lithium ion batteries and in corrosion prevention (Allia 2013, Xu 2013, Cardillo 2013).

The three important crystallographic phases of iron oxide include: 1) magnetite (Fe_3O_4); 2) maghemite (γ-Fe_2O_3) and 3) hematite (α-Fe_2O_3) (Akbar 2014 (a), Riaz 2013). Among these phases of iron oxide, hematite is widely used in magnetic recording media, as a catalyst, gas sensors etc. These applications of iron oxide arise due to its low cost, thermal stability, its resistance to corrosion and its non-toxic nature.

In bulk, hematite exhibits antiferromagnetic behavior below temperature of 260K. This temperature is known as Morin temperature. Above this temperature, hematite exhibits weak ferromagnetic behavior. In hematite spins in neighboring planes are

[1), 2)] Professor

antiferromagnetically coupled. Spins in same plane have ferromagnetic coupling between them (Saeed 2013, Akbar 2014(b)).

In order to enhance the magnetic properties of hematite, various dopants have been reported in literature including Ti (Wang 2009), Co (Suresh 2012), Al (Shinde 2011), Cr (Yogi 2013) etc. Among these dopants cobalt, with electronic configuration of $[Ar]3d^7 4s^2$ has one more electron than iron, has gained much attention. Cobalt atom donates one d and two s electrons to oxygen that results in remaining six electrons on cobalt. When Co is substituted for Fe with spin down electron the spin down d band gets completely filled with remaining one d-electron residing in spin up band. This results in increase in net magnetization in cobalt doped iron oxide.

We here report the structural and magnetic properties of hematite cobalt doped nanoparticles prepared using sol-gel method. The dopant concentration is varied as 2-10%. Changes in structural and magnetic are correlated with dopant concentration.

2. EXPERIMENTAL DETAILS

Cobalt doped iron oxide nanoparticles (NPs) were prepared using sol-gel method. $Fe(NO_3)_3.9H_2O$ was dissolved in deionized (DI) water. The solution was stirred at room temperature. Ethylene glycol was added to the above solution. The solution was then heated on hot plate at 80˚C to obtain undoped and cobalt doped iron oxide nanoparticles. Details of sol-gel synthesis are reported earlier (Akbar 2014(a)).

NPs were characterized structurally using Bruker D8 Advance X-ray Diffractometer with Cukα=1.5406Å. Magnetic properties of undoped and cobalt doped NPs were studied with Lakeshore's 7407 vibrating sample magnetometer.

3. RESULTS AND DISCUSSION

Fig. 1 shows XRD pattern for undoped iron oxide nanoparticles prepared using sol-gel method. The presence of diffraction peaks corresponding to planes (102), (104), (110), (113), (024), (116), (214) and (300) indicate the formation of pure hematite phase. XRD patterns for cobalt doped iron oxide are shown in Fig. 2. No peaks corresponding to cobalt and/or cobalt oxide were observed indicative of successful incorporation of cobalt in the host lattice. The peak positions corresponding to planes (202) and (024) shifted to slightly higher angles. The shift of peak positions to high angles is attributed to smaller ionic radius of cobalt as compared to that of iron. This will lead to shrinkage of unit cell thus reducing the d-spacing. Reduction in d-spacing, according to Bragg's law (Cullity 1956), shifts the peak positions to higher diffraction angles (Fig. 2).

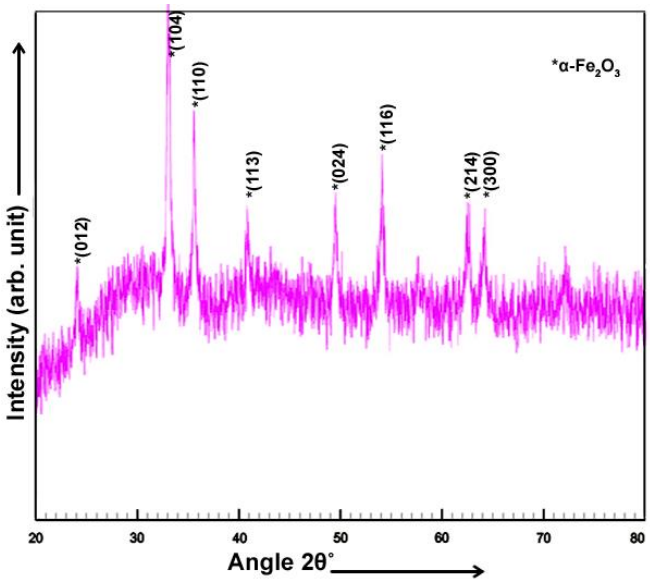

Fig. 1 XRD pattern for undoped iron oxide nanoparticles

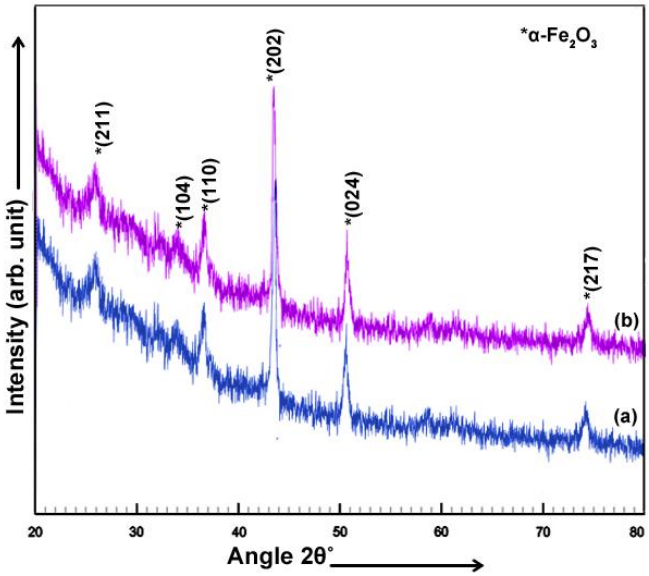

Fig. 2 XRD patterns for cobalt doped iron oxide nanoparticles with dopant concentration (a) 2% (b) 6%

Crystallite size (t) and dislocation density (δ) (Cullity 1956) of cobalt doped iron oxide nanoparticles was calculated using Eq. (1)-(2)

$$t = \frac{0.9\lambda}{B\cos\theta} \quad (1)$$

$$\delta = \frac{1}{t^2} \quad (2)$$

Where, λ is the wavelength (1.5406Å), B is the Full Width at Half Maximum (FWHM). Crystallite size and dislocation density are plotted as a function of dopant concentration in Fig. 3. Crystallite size increases from 23nm for undoped iron oxide nanoparticles to

26.5nm for 2% doping. Increasing the dopant concentration to 6% resulted in increase in crystallite size to 32.5nm. For dopant concentration of 10%, crystallite size was reduced to 28.1nm. Decrease in crystallite size at dopant concentration of 10% can be attributed to presence of amorphous impurities at the grain boundaries that increases the dislocation density to 12.7×10^{14} lines/m^2. As the result of presence of amorphous impurities at grain boundaries the reduction in crystallite size was observed.

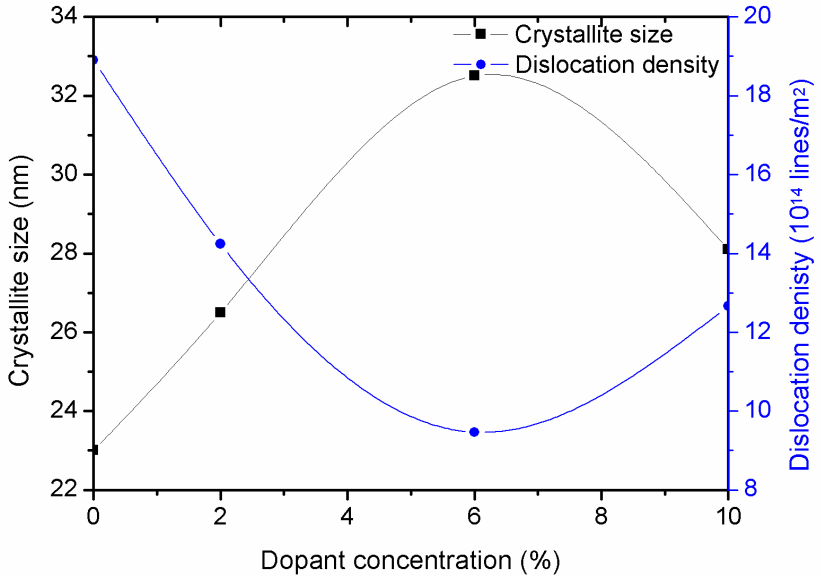

Fig. 3 Crystallite size and dislocation density as a function of dopant concentration

Lattice parameter, unit cell volume of cobalt doped iron oxide nanoparticles were calculated using Eq. 3 and 4 and are listed in table 1.

$$\sin^2\theta = \frac{\lambda^2}{3a^2}\left(h^2+k^2+hk\right)+\frac{\lambda^2 l^2}{4c^2} \quad (3)$$

$$\rho = \frac{1.66042\ \Sigma A}{V} \quad (4)$$

Where, *(hkl)* represent the miller indices, ***ΣA*** is the sum of atomic weights of the atoms in the unit cell, *V* is the volume of unit cell (V=0.866a^2c).

Table 1 Structural properties of cobalt doped iron oxide nanoparticles

Dopant concentration (%)	Lattice parameter (Å)		Unit cell volume (Å^3)	X-ray density (g/cm^3)
	a	c		
0	5.04	13.69	301.1497	5.26217
2	5.03	13.62	298.4221	5.310266
6	5.01	13.59	295.4016	5.364564
10	4.99	13.52	291.5383	5.435651

The decrease in lattice parameters and unit cell volume is observed with increase in dopant concentration due to smaller ionic radius of cobalt as compared to that of iron.

Shrinkage of the unit cell was observed with increasing dopant concentration that leads to reduction in lattice parameters *a* and *c*. Cobalt doped iron oxide nanoparticles show density in the range of 291-301g/cm^3.

Fig. 4 show room temperature M-H curves for cobalt doped iron oxide nanoparticles. with increase in dopant concentration to 6% saturation magnetization increases from 7×10^{-4} emu to 1.1×10^{-3} emu. Further increase in dopant concentration resulted in reduction in saturation magnetization to 6.7×10^{-4} emu.

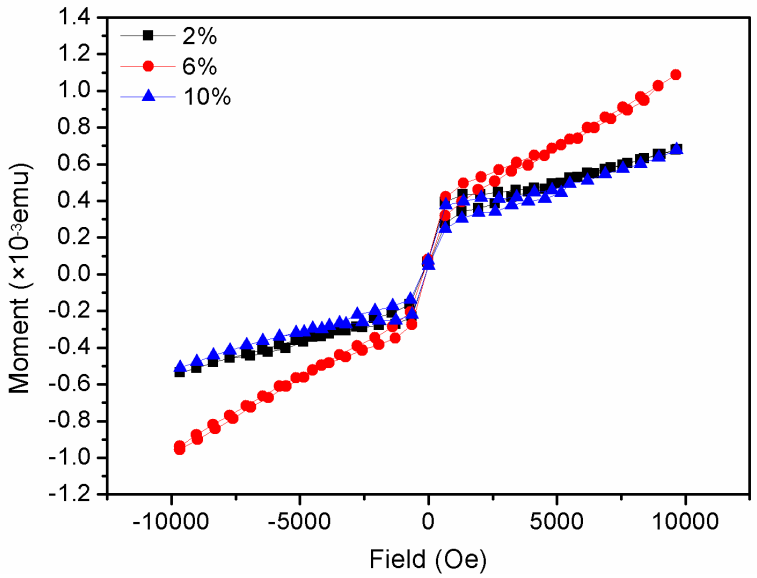

Fig. 4 M-H curves for cobalt doped iron oxide nanoparticles

Hematite is antiferromagnetic in nature with Neel temperature of 955K exhibiting insulating properties. Below temperature of 260K shows a transition from antiferromagnetic to weak ferromagnetic behavior. This transition in magnetic properties arises due to canting in the magnetization of two sublattices in hematite crystal structure. Due to spin orbit coupling canting between two adjacent planes arises that produces uncompensated magnetic moment of Fe^{3+} cations. Thus, weak ferromagnetic or canted ferromagnetic behavior arises in otherwise antiferromagnetic hematite. In hematite, the spins in the adjacent planes are ferromagnetically coupled where antiferromagnetic coupling arises with the spins of the adjacent planes. Spin orbit coupling between the two adjacent planes give rise to uncompensated spins of Fe^{3+} cations. These uncompensated spins produced the canting of spins between the planes that is the cause of ferromagnetic behavior in other antiferromagnetic material. Effect of cobalt doping on saturation magnetization, coercivity, S* and squareness can be seen in table 2.

Cobalt with electronic configuration of $[Ar]3d^74s^2$ has one more electron than iron. Cobalt atom donates one d and two s electrons to oxygen that results in remaining six electrons on cobalt. When Co is substituted for Fe with spin down electron the spin down d band gets completely filled with remaining one d-electron residing in spin up band. This results in increase in net magnetization in cobalt doped iron oxide nanoparticles as compared to undoped iron oxide nanoparticles. In addition, as it was

observed in Fig. 3 that with increase in dopant concentration to 6% the crystallite size increases. This increase in crystallite size to 32nm also resulted in increase in saturation magnetization.

Table 2 Magnetic properties of cobalt doped iron oxide nanoparticles

Dopant concentration (%)	Saturation magnetization M_S (10^{-3} emu)	Coercivity (Oe)	Retentivity M_r (10^{-6} emu)	Squareness	S*
2	0.7	61.0	16.7	0.027	0.37
6	1.1	56.2	19.2	0.018	0.32
10	0.67	73.8	18.06	0.03	0.41

4. CONCLUSIONS

Cobalt doped iron oxide nanoparticles were prepared using sol-gel method. The dopant concentration is varied at 2%, 4%, 6%, 8% and 10%. Presence of diffraction peaks corresponding to planes (102), (104), (110), (113), (024), (116), (214) and (300) indicated the formation of hematite phase of iron oxide. The peak positions corresponding to hematite shifted to higher angles with increase in dopant concentration. Crystallite size increases from 23nm to 32nm with increase in dopant concentration to 6%. Ferromagnetic behavior in cobalt doped iron oxide nanoparticles due to spin orbit coupling between adjacent planes. Saturation magnetization of 7×10^{-4} emu, 1.1×10^{-3} emu and 6.7×10^{-4} emu was observed with dopant concentration of 2%, 6% and 10% respectively.

REFERENCES

Akbar, A., Riaz, S., Ashraf, R. and Naseem, S. (2014(b)), "Magnetic and magnetization properties of Co-doped Fe_2O_3 thin films," *IEEE Trans. Magn.*, doi: 10.1109/TMAG.2014.2311826

Akbar, A., Riaz, S., Bashir, M. and Naseem, S. (2014(a)), "Effect of Fe^{3+}/Fe^{2+} ratio on superparamagnetic behaviour of spin coated iron oxide thin films," *IEEE Trans. Magn.*, doi: 10.1109/TMAG.2014.2312972.

Allia, P., Barrera, G., Bonelli, B., Freyria, F.S. and Tiberto, P. (2013), "Magnetic properties of pure and Eu-doped hematite nanoparticles," *J. Nanopart. Res.*,**15**, 2118.

Cardillo, D., Konstantinov, K. and Devers, T. (2013), "The effects of cerium doping on the size, morphology, and optical properties of α-hematite nanoparticles for ultraviolet filtration," *Mater. Res. Bull.*, **48**, 4521–4525

electrochemical sensing properties," *Mater. Chem. Phys.*, **134**, 590-596

Kamali, S., Shahmiri, N., Garitaonandia, J.S., Ångström, J., Sahlberg, M., Ericsson, T., Haggstrom, L. (2013), "Effect of mixing tool on magnetic properties of hematite nanoparticles prepared by sol–gel method," *Thin Solid Films*, **534**, 260–264.

Khalil, M., Yu, J., Liu, N. and Lee, R.L. (2014), "Hydrothermal synthesis, characterization, and growth mechanism of hematite nanoparticles," *J. Nanopart. Res.*, **16**, 2362.

Shinde, S.S., Moholkar, A.V., Kim, J.H. and Rajpure, K.Y. (2011), "Structural, morphological, luminescent and electronic properties of sprayed aluminum incorporated iron oxide thin films," *Surf. Coat. Technol.*, **205**, 3567–3577.

Suresh, R., Prabu, R., Vijayaraj, A., Giribabu, K., Stephen, A. and Narayanan, V. (2012), "Facile synthesis of cobalt doped hematite nanospheres: Magnetic and their

Wang, B., Song, Y., Ren, W., Xu, W. and Cui, H. (2009), "Low temperature transformation from γ-Fe_2O_3 to Ti doped α-Fe_2O_3 nanoparticles through an epoxide assisted sol–gel route," *J. Sol-Gel Sci. Technol.*, **51**, 119–123.

Xu, Y., Zhang, G., Du, G., Sun, Y. and Gao, D. (2013), "α-Fe_2O_3 nanostructures with different morphologies: Additive-free synthesis, magnetic properties, and visible light photocatalytic properties," *Mater. Lett.*, **92**, 321–324.

Yogi, A. and Varshney, D. (2013), "Magnetic and structural properties of pure and Cr-doped hematite: α-$Fe_{2-x}Cr_xO_3$ ($0 \le x \le 1$)," *J. Adv. Ceram.*, **2**, 360-369.